

New precise dating of the India-Asia collision in the Tibetan Himalaya at 61 Ma

Wei An^{1,2}, Xiumian Hu^{2*}, Eduardo Garzanti³, Jian-Gang Wang⁴ and Qun Liu²

¹School of Resources and Environmental Engineering, Hefei University of Technology, Hefei 230009, China

²State Key Laboratory of Mineral Deposits Research, School of Earth Sciences and Engineering, Nanjing University, Nanjing 210023, China

³Department of Earth and Environmental Sciences, Università di Milano-Bicocca, Milano, 20126, Italy

⁴State Key Laboratory of Lithospheric Evolution, Institute of Geology and Geophysics, Chinese Academy of Sciences, Beijing 100029, China

*E-mail: huxm@nju.edu.cn

Key Points:

- The newly reported Mubala section records Indian-passive-margin and Transhimalayan-trench strata related to the India-Asia collision.
- The India-Asia provenance reversal has been bracketed between 62.7 to 61 Ma in the Mubala section.
- The initial India-Asia collision is constrained no later than 61 Ma in the Tibetan Himalaya.

Abstract

The timing of the India-Asia collision onset, essential to understand the evolution of the Himalayan-Tibetan orogen, has been widely investigated through multidisciplinary approaches, among which the India to Asia provenance reversal documented in the Indian passive margin successions was proved to be most effective. We present integrated stratigraphic, sedimentological, and provenance data on Paleocene strata from the newly investigated Mubala section south of the Yarlung-Zangbo suture zone in southern Tibet, which preserves continuous deep-marine turbiditic and biogenic sedimentation on the distal northern Indian passive margin. Sandstone petrography, heavy minerals, detrital zircon geochronology and Hf isotopes, and detrital Cr-spinel geochemistry diagnose the Indian to Asian provenance reversal bracketed between 62.7 Ma by the youngest zircon ages from the earliest Asian-derived sandstone and 61.0 ± 0.3 Ma by SIMS age of a tuffaceous layer ~30 m above this bed. Thus, the collision onset is constrained most probably around 61 Ma in the Tibetan Himalaya.

Plain Language Summary

The India-Asia collision, leading to uplift of the Himalayan range and Tibetan plateau, has greatly influenced Cenozoic climate, oceanic circulation, and faunal changes. The timing of collision is essential to model the topographic evolution of the Himalayan-Tibetan orogen and its environmental and paleogeographic effects, and has been widely investigated through multidisciplinary approaches. The sediment provenance change along the Indian continental margin was proved to be a most effective method. We report a new section deposited at the deep-marine Indian continental margin recording the India to Asia provenance change in south Tibet. The provenance change was constrained between 62.7 Ma by the youngest zircon ages from the earliest Asian-derived sandstone and 61.0 ± 0.3 Ma by SIMS age of a tuffaceous layer above this bed. This study suggests the India-Asia collision around 61 Ma in the Tibetan Himalaya.

1. Introduction

The India-Asia collision induced rapid uplift of the Tibetan Plateau and affected global atmospheric and oceanic circulation throughout the Cenozoic (An et al., 2001; Molnar et al., 2010). Geological records from both the northern India and the Yarlung-Zangbo suture zone (YZSZ) indicate a Paleogene collision event, interpreted as India colliding with an intra-oceanic arc (Aitchison et al., 2000, 2007) or with Asia (Ding et al., 2005; DeCelles et al., 2014; Hu et al., 2015). However, the latter has been favored in Tibetan segment as no record of intra-oceanic arc or arc-continental collision exists (Hu et al., 2016).

Multidisciplinary efforts have been spent to determine the timing of initial collision, a key parameter to understand the subsequent evolution of the Himalayan-Tibetan orogen and its global consequences (e.g., Beck et al., 1995; Yin and Harrison, 2000; Ding et al., 2005; Leech et al., 2005). Previous studies documented that the India to Asia provenance reversal (IAPR) recorded in sandstones deposited on the Indian passive margin represents a fundamental clue to constrain the time of collision onset (Garzanti et al., 1987; Najman et al., 2010, 2017; Hu et al., 2016). The age of this major geological event can be most precisely pin-pointed in deep-water turbiditic successions deposited on the northern edge of the Indian margin (Wang et al., 2011; DeCelles et al., 2014; Wu et al., 2014; Hu et al., 2015).

The Sangdanlin section in Tibet, south of YZSZ, has been well studied for this purpose. The determination of nannofossil assemblages from strata ~100 m above the IAPR and of radiolarian assemblages both below and above the IAPR (Hu et al., 2015), combined with detrital-zircon chronostratigraphy (immediately above the IAPR; Wang et al., 2011; DeCelles

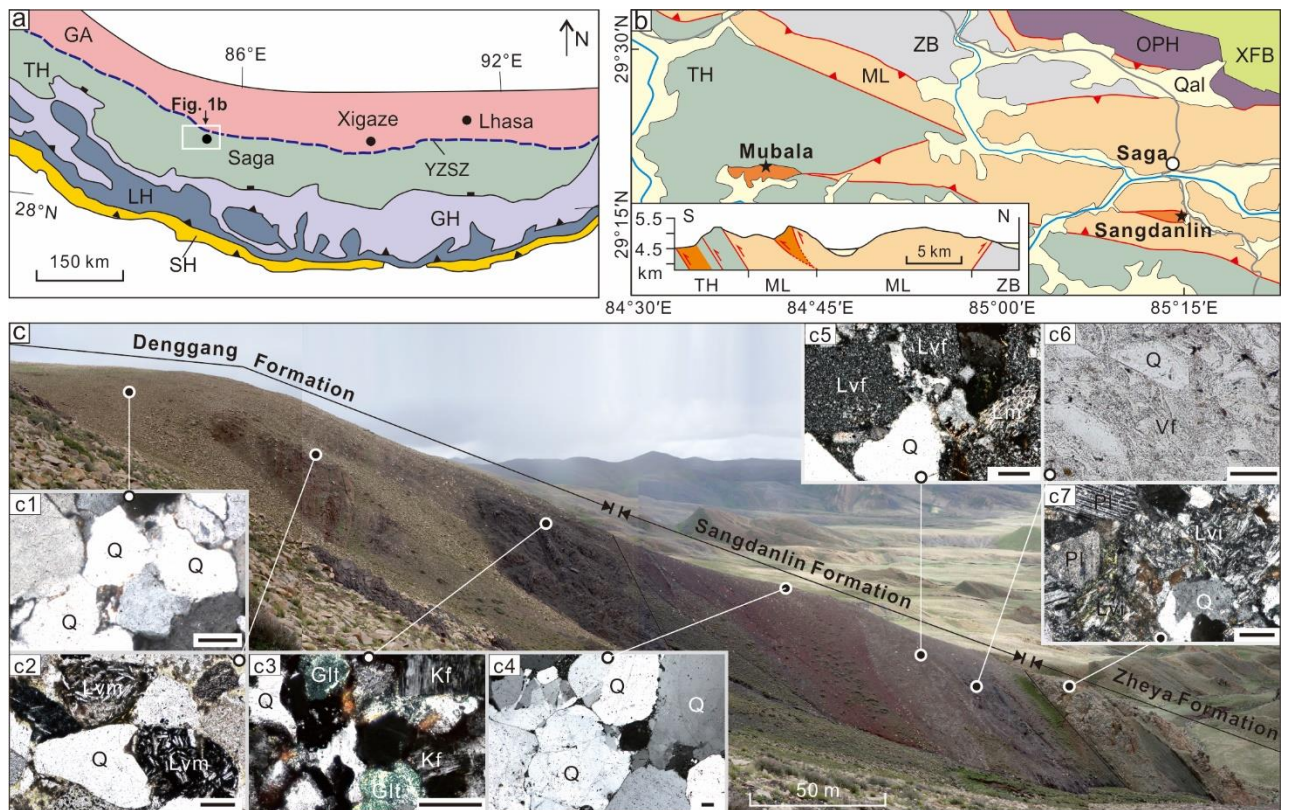
et al., 2014; Wu et al., 2014) and with zircon ages in tuff layer ~510 m above the IAPR (DeCelles et al., 2014) have constrained the India-Asia collision onset as 59 ± 1 Ma (Hu et al., 2015). However, all of these methods are subject to minor inaccuracies. The nannofossils-bearing beds and the tuff layer are younger than the IAPR, the time range of radiolarian biozones is not precisely determined, and stratigraphic or tectonic discontinuities may occur (Chan, 2006; Li et al., 2007). Moreover, one section is insufficient to establish the age of such a prominent geological event conclusively. Therefore, more stratigraphic sections are needed to constrain collision onset with additional accuracy and precision, and to quantify its potential diachrony along strike.

In this study we provide new stratigraphic, petrographic, heavy-mineral, geochronological and geochemical data from stratigraphically continuous Paleocene strata of the Mubala section south of the YZSZ in southern Tibet (Fig.1a, 1b). The Mubala section preserves the northernmost and earliest record of transition between Indian-passive-margin and Transhimalayan-trench sedimentation associated with the India-Asia collision. Our new data constrain collision onset around 61 Ma at Mubala section in the Tibetan Himalaya.

2. Geological Setting

The Mubala section is located ~65 km southwest of Saga in Tibet (Fig.1a, 1b) and situated south of the Yarlung-Zangbo suture zone formed during the Cenozoic India-Asia collision. The Yarlung-Zangbo suture zone consists the mid-Cretaceous to late Miocene Gangdese magmatic arc, Aptian-Paleocene Xigaze forearc basin filled with marine to nonmarine sediments and the accretionary prism of mud- and serpentinite-matrix mélangé and

89 subduction complex accreted to the southern margin of Asia (Garzanti et al., 1987; Burg et al.,
 90 1987). To the south, the northern Tethyan Himalaya zone comprises Late Paleozoic to
 91 Cretaceous strata, representing the northern Indian passive margin, overlaid by siliciclastic
 92 sedimentary rocks deposited in foreland basin of the India-Asia collision (e.g., Garzanti et al.,
 93 1987; DeCelles et al., 2014; Hu et al., 2015).



95 **Figure 1.** The Mubala section in southern Tibet. **a)** Geological sketch map of the southern
 96 Lhasa terrane and Himalayan belt; **b)** Simplified geological map and cross-section of the Saga
 97 area (based on Pan et al., 2004, Hu et al., 2016, Metcalf and Kapp, 2017, and own field
 98 observations). Locations of the Mubala and Sangdanlin sections are shown by stars.
 99 GA-Gangdese magmatic arc; YZSZ-Yarlung-Zangbo suture zone; TH-Tethys Himalaya;
 100 GH-Greater Himalaya; LH-Lesser Himalaya; SH-Subhimalaya; XFB-Xigaze forearc basin;

OPH-Ophiolite; ZB-Zhongba terrane; ML-Xiukang complex; Qal-Quaternary. c) Panorama of the Mubala section exposing the studied stratigraphic units: India-derived quartzose (c1) and quartzo-lithic basalticlastic (c2) sandstones of the lower and middle Denggang Fm.; glaucony-bearing feldspatho-quartzose (c3) and quartzose (c4) sandstones of the upper Denggang and lower Sangdanlin Fms.; Asia-derived feldspatho-litho-quartzose volcanoclastic sandstone (c5) and interbedded tuff layers (c6) of the upper Sangdanlin Fm.; sandstone (c7) of the Zheya Fm. Q - quartz; Pl - plagioclase; Kf - K-feldspar; Lvm, Lvi, Lvfi - mafic, intermediate and felsic volcanic lithics; Lm - metamorphic lithics; Glt - glaucony; Vf - vitric fragments; 100 μ m bar for scale.

3. Stratigraphy

The Mubala section (Fig. 1c) was measured bed-by-bed. The 330 m-thick siliciclastic succession conformably overlies dark grey siliceous shale interbedded with chert of the Jiabula Formation within the northern Tethys Himalayan zone (Li et al., 2005). The succession can be subdivided into three parts with conformable stratigraphic contacts featured by distinct lithological changes, correlating with the Denggang, Sangdanlin, and lower Zheya formations in the Sangdanlin section (Fig. 1c, Fig. 2).

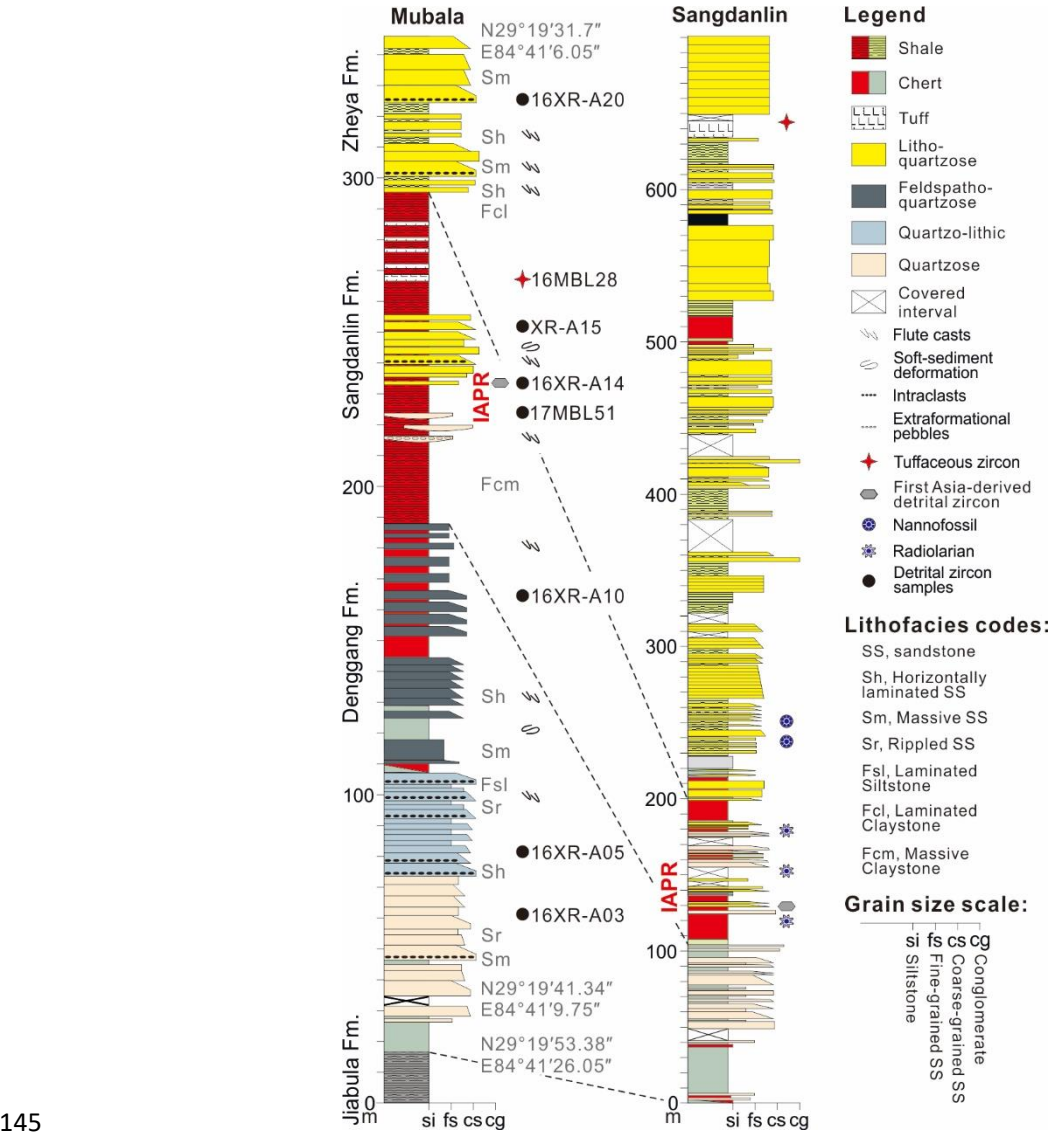
The Denggang Formation (160 m-thick), consisting of siliceous shales, chert, siltstone and sandstone, is divided into three members. The lower member (60 m-thick) consists of green siliceous shales passing upward to thick-bedded, medium to coarse-grained sandstone (Fig. 1c1). The middle brown member (30 m-thick) consists of 0.1-1.5 m-thick, fine- to coarse-grained sandstone intercalated with siltstone (Fig. 1c2). The upper member (70 m thick)

consists of dark green, 0.1-0.6 m-thick, fine-grained sandstone (Fig. 1c3) interbedded with green/purple radiolarian chert and purple siliceous shales. The lower member correlates with Units 1-8 of the Sangdanlin section, whereas the middle and upper members with Units 9-10 (DeCelles et al., 2014; Hu et al., 2015). Sandstone beds display erosional base, flute casts, parallel or ripple lamination, and common intraclasts, indicating deposition from turbidity currents. Thick and coarse-grained beds in the lower and middle members were deposited by high-density flows, whereas thinner beds in the upper member document low-density flows intercalated with background biogenic deposits (Mutti, 1992).

The Sangdanlin Formation (120 m-thick) includes two members in the Mubala section. The lower member (50 m-thick) includes purple siliceous shale intercalated with purple radiolarian chert and lenticular sandstone (Fig. 1c4). The upper member includes 30 m of thin- to medium-bedded, medium- to coarse-grained sandstone (Fig. 1c5) overlain by 40 m of purple siliceous shale intercalated with numerous thin-bedded tuff layers (Fig. 1c6). The lower member correlates with Units 11-13 of the Sangdanlin section, whereas the upper member is similar to Units 14-21. Radiolarian chert and siliceous shale indicate biogenic deposition at abyssal depths during periods of reduced clastic influx. Sandstone beds showing flute and groove casts, parallel and ripple lamination, graded-bedding, or erosional base indicate deposition from distal turbidity currents.

The Zheyu Formation (50 m) in the Mubala section consists of thin- to thick-bedded, medium-grained to pebbly sandstones with upward-decreasing grey shale intercalations (Fig. 1c7), corresponding to Units 22-26 of the Sangdanlin section. Parallel or ripple lamination,

143 graded-bedding, erosional base, load or flute casts and intraclasts are common, suggesting
 144 deposition by high-density turbidity currents.



145 **Figure 2.** Stratigraphic column of the Mubala section correlated with the Sangdanlin section
 146 exposed ~60 km to the east. The position of sandstone and tuff samples dated by zircon U-Pb
 147 geochronology and of samples dated by biostratigraphy are indicated. The occurrence of the
 148 India-Asia provenance reversal (IAPR) is indicated in red.

150 4. Methods and Sampling

Fifteen sandstone samples collected throughout the Mubala section were point-counted; heavy-mineral analysis was carried out on nine of them. Cr-spinels were separated from 4 samples from the Denggang and upper Sangdanlin formations. Detrital zircons from 7 samples yielded 574 concordant U-Pb ages, 237 Cenozoic-Mesozoic ones of which were analyzed for Hf isotopes. Thirty-six ages were obtained from the tuff in the upper Sangdanlin Formation. See Supporting information for detailed analytical procedures and complete datasets.

5. Results

In the Denggang Formation, sandstones are quartzose in the lower member, litho-quartzose to quartzo-lithic basalticlastic in the middle member, and glaucony-bearing feldspatho-quartzose in the upper member (Fig. 3a). In the Sangdanlin Formation, sandstones are quartzose in the lower member and feldspatho-litho-quartzose volcanoclastic in the upper member as in the overlying Zheya Formation (Fig. 3a). Heavy minerals document an upward decrease in durable zircon, tourmaline and rutile (ZTR index; Hubert, 1962). Garnet and apatite characterize the Denggang and lower Sangdanlin formations, whereas epidote is dominant in the upper Sangdanlin and Zheya formations. Cr-spinels from the middle and upper Denggang Formation have higher TiO₂ contents than those from the Sangdanlin Formation (Fig. 3b).

Detrital zircons from the lower and middle Denggang Formation exhibit prominent age clusters at 500-570 Ma (peaks at ~522 and ~567 Ma) and 800-1000 Ma (peak at ~950 Ma) with subordinate older ages (Fig. 3c). Detrital zircons from the upper Denggang and lower

Sangdanlin formations display similar age spectra, with an additional cluster at 115-150 Ma (peaks at ~128 and 138 Ma) characterized by negative $\epsilon_{\text{Hf}}(t)$ values (Fig. 3d). In contrast, the upper Sangdanlin and Zheyu formations yielded mainly Cenozoic-Mesozoic ages (Fig. 3c), with clusters at 60-70 Ma and 80-120 Ma and mainly positive $\epsilon_{\text{Hf}}(t)$ values (Fig. 3d).

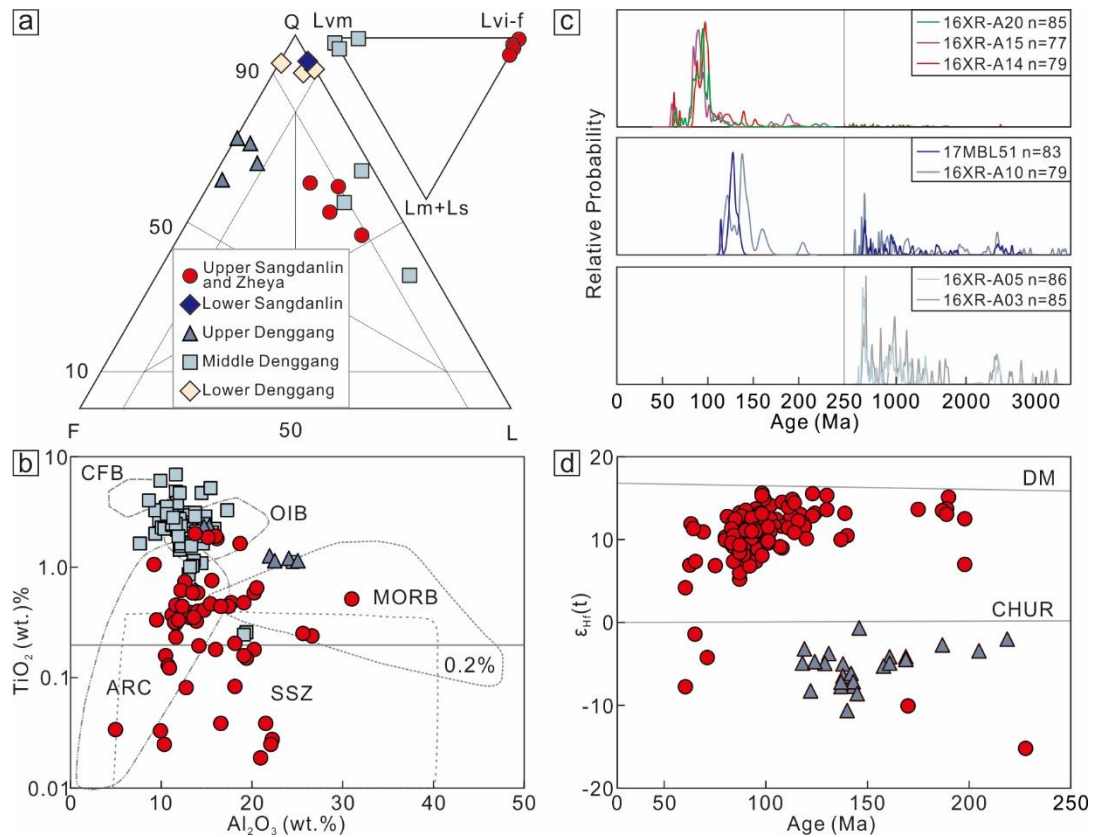


Figure 3. Provenance data from the Mubala section. **a)** Petrography. Compositional fields in the QFL plot (Q= quartz; F= feldspars; L= lithics) after Garzanti (2019). Lm+Ls= metamorphic and sedimentary lithics; Lv_m and Lv_{i-f}= mafic and intermediate + felsic volcanic lithics. **b)** Geochemistry of detrital Cr-spinel. Compositional fields after Kamenetsky et al. (2001): CFB = continental-flood basalts; OIB = oceanic-island basalts; MORB = mid-ocean-ridge basalts. **c)** U-Pb age spectra of detrital zircons. **d)** Hf isotopic signature of Mesozoic zircons. All data available in Supplementary Tables S1-S4.

6. The India-Asia Provenance Reversal

Petrographic, heavy-mineral, and geochronological data document multistep changes in provenance through the Mubala section. Quartzose sandstones with high ZTR index in the lower Denggang Formation were derived from cratonic interiors, whereas abundant basaltic detritus in the middle member was sourced from mafic lavas. The Sangdanlin Formation documents a provenance change from quartzose sandstones derived from cratonic interiors in the lower member, to volcaniclastic sandstones with abundant plagioclase and epidote from a magmatic arc in the upper member.

These provenance interpretations are supported by detrital zircon ages, Hf isotopes and Cr-spinel geochemistry. The Denggang and lower Sangdanlin sandstones are dominated by Early Cretaceous zircons with negative $\epsilon\text{Hf}(t)$ values and pre-490 Ma ages, matching well with those from Tethys Himalayan strata (Hu et al., 2010; Gehrels et al., 2011; DeCelles et al., 2014). High TiO_2 content in Cr-spinels is also similar to those in Tethys Himalayan strata (Hu et al., 2014). Conversely, the predominant Cenozoic-Mesozoic zircons with positive $\epsilon\text{Hf}(t)$ values and low TiO_2 Cr-spinels from the upper Sangdanlin and Zheya formations indicate dominant provenance from the Gangdese magmatic arc (Ji et al., 2009; DeCelles et al., 2014; Hu et al., 2014, 2015).

Quartzose sandstones in the lower Denggang Formation were derived from the Indian shield, whereas quartzo-lithic basalticlastic sandstones in the middle Denggang Formation most likely testify to the main outburst of Deccan volcanism close to the Cretaceous/Tertiary boundary (e.g., Chenet et al., 2007; Li et al., 2020). The glaucony-rich feldspatho-quartzose

sandstones of the upper Denggang Formation may reflect dissection of the Deccan lava pile in central–northern India and reworking of the underlying Upper Cretaceous including glaucony-bearing feldspatho-quartzose sandstones (e.g., Bansal et al., 2018). Glaucony-bearing sandstones are also found at the top of the lower Paleocene Stumpata and Jidula formations of the Tethys Himalaya, reflecting a period of reduced subsidence and starved sedimentation (Nicora et al., 1987; Garzanti and Hu, 2015). The occurrence of Early Cretaceous detrital zircons in the upper Denggang and lower Sangdanlin formations indicate further deepening of erosion into Lower Cretaceous volcanic rocks of the Indian margin and possibly older Tethys Himalaya strata (Hu et al., 2010).

The IAPR occurs between the lower and upper Sangdanlin Formation, and is a direct testimony of India-Asia collision onset (DeCelles et al., 2014). In the Mubala section, the IAPR corresponds to an abrupt single change from quartzose to feldspatho-litho-quartzose volcanoclastic sandstone, whereas Indian-derived and Asian-derived turbidites are intercalated through much of the central part of the Sangdanlin Formation in the Sangdanlin section (Wang et al., 2011).

A maximum age constraint to the IAPR is provided by the youngest age cluster of detrital zircons from the first Asia-derived sandstone, displaying a prominent peak at 62.7 Ma (Fig.3B). A firmer age constraint is provided by the SIMS age of 61.0 ± 0.3 Ma of the tuff layer interbedded ~30 m above the first Asia-derived sandstone (Fig.4a, 4b). The IAPR in the Mubala section is therefore robustly bracketed between 62.7 Ma and 61.0 ± 0.3 Ma. This age interval appears to be a bit older than the pre-58.5 Ma (DeCelles et al., 2014) and 59 ± 1 Ma

(Hu et al., 2015) from the Sangdanlin section. The apparent discrepancy may be largely ascribed to the closer position of the Mubala tuff to the IAPR (~30 m above) than the Sangdanlin tuff (~510 m above) (Fig. 4c).

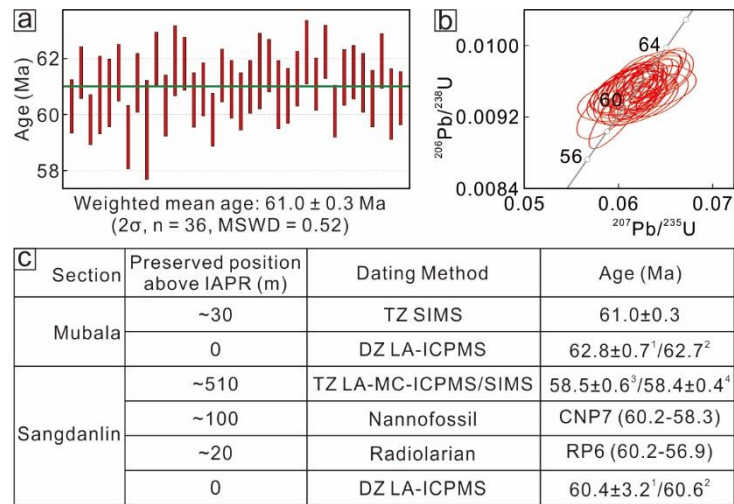


Figure 4. Dating the IAPR with different methods. **a, b)** Age plots for the tuff intercalated 30 m above the base of the upper Sangdanlin Fm. **c)** Comparison between chronostratigraphic data obtained from the Mubala and Sangdanlin sections (after DeCelles et al., 2014, Hu et al., 2015, and this study): 1, weighted mean age for the youngest cluster of zircon grains; 2, peak age of the youngest cluster of zircon grains; 3, LA-MC-ICPMS zircon ages; 4, SIMS zircon ages. All data available in Supplementary Tables S5.

7. Timing of the India-Asia Collision

The onset of continental collision is most aptly defined as the moment when two continents come into physical contact (Beck et al., 1995; DeCelles et al., 2014; Hu et al., 2016, 2017). Various methods have been used to estimate the time of India-Asia collision, among which the coupled stratigraphic/sediment provenance approach has been demonstrated to provide the direct estimate (e.g., Garzanti et al., 1987; Rowley, 1996; Hu et al., 2016). The

superposition of Asian-derived turbidites onto Indian-derived turbidites in the Mubala section, however, might have occurred somewhat earlier than actual collision onset. The Transhimalayan trench may have been overfilled, and thus bypassed by turbiditic flows spreading oceanward. In the heavily sediment-filled trench of south-central Chile, for instance, turbiditic deposits extend as far as 250 km seaward of the trench axis (Contreras-Reyes et al., 2010). Considering the rapid convergence rate of India and Asia in the early Paleocene (150 km/Ma, Copley et al., 2010), even in such an overfilled-trench scenario the onset of collision between two continents should be quite close to 61 Ma.

The importance of the Mubala section also resides in the fact that it rests stratigraphically on top of Tethys Himalayan strata, proving that deposition took place onto the distal edge of the Indian passive margin. If the trench was incompletely filled and represented a barrier to turbiditic transport, then the IAPR must coincide in time with collision onset, which would thus be constrained between the youngest detrital zircon ages in the oldest Asian-derived sandstone (62.7 Ma), and age of the tuff intercalated ~30 m above the IAPR (61.0 ± 0.3 Ma).

Plate circuit reconstructions suggest >4000 km of convergence since 60 Ma whereas the estimated upper crustal shortening amounts are ~2000 km, a discrepancy leading to the putative “Greater India basin” (van Hinsbergen et al., 2012), “north India sea” (Yuan et al., 2020) or “Xigaze backarc basin” (Kapp and DeCelles, 2019). However, sandstone from the Denggang Formation with detritus from Deccan Traps and underlying strata indicates sediments transportation from the central-northern India craton to the Tethyan Himalaya, precluding an intervening oceanic basin. Meanwhile, Cr-spinel from the Sangdanlin and

Zheya formations display identical compositions to those from the Xigaze forearc basin (Hu et al., 2014), suggesting no major change in provenance before and after the proposed 90-60 Ma Xigaze backarc basin.

8. Conclusion

The Mubala section consists of turbiditic and abyssal sediments deposited onto the Indian continental rise (Denggang and lower Sangdanlin formations) and in the Transhimalayan trench (upper Sangdanlin and Zheya formations). Several provenance changes are recorded in the Denggang and lower Sangdanlin formations, indicating erosion of the Indian shield before, during, and after the major outburst of Deccan continental flood basalts. The major provenance reversal from India to Asia occurred at the boundary between the lower and upper Sangdanlin Formation, and is bracketed between 62.7 Ma (youngest detrital zircons in the oldest Asian-derived sandstone) and 61.0 ± 0.3 Ma (age of the tuff intercalated ~30 m above). Our data indicate that the continental margins of India and Asia first engaged in collision very close to 61 Ma at Mubala locality (early Selandian). This is believed to represent the most accurate direct age constraint ever obtained on the age of the India-Asia collision so far.

Acknowledgments

We thank Hanpu Fu, Weiqiang Ji, and Xiaoping Xia for their assistance in the field and in the laboratory, Mara Limonta and Wendong Liang for heavy-mineral analyses, and Heinrich Bahlburg, Fuyuan Wu for fruitful discussion. This study was supported financially by the National Science Foundation of China (projects 91755209, 41972106), the State Key

Laboratory of Mineral Deposits Research, Nanjing University (2018-LAMD-K01) and China
Postdoctoral Science Foundation (Grant No. 2019M662136). Supporting figures and data are
provided in Figure S1-S3 and Table S1-S6.

References

- Aitchison, J. C., Ali, J. R., & Davis, A. M. (2007). When and where did India and Asia collide?
Journal of Geophysical Research-Solid Earth, 112, B05423. doi:10.1029/2006JB004706
- Aitchison, J. C., Badengzhu, Davis, A. M., Liu, J. B., Luo, H., Malpas, J. G., McDermid, I. R. C.,
Wu, H. Y., Ziabrev, S. V., & Zhou, M. F. (2000). Remnants of a Cretaceous intra-oceanic
subduction system within the Yarlung-Zangbo suture (southern Tibet). *Earth and Planetary
Science Letters*, 183(1-2), 231-244.
- An, Z., Kutzbach, J. E., Prell, W. L., & Porter, S. C. (2001). Evolution of Asian monsoons and
phased uplift of the Himalaya-Tibetan plateau since Late Miocene times. *Nature*,
411(6833), 62-66.
- Bansal, U., Banerjee, S., Ruidas, D. K., & Pande, K. (2018). Origin and geochemical
characterization of the glauconites in the Upper Cretaceous Lameta Formation, Narmada
Basin, central India. *Journal of Palaeogeography*, 7(2), 99-116.
- Beck, R. A., Burbank, D. W., Sercombe, W. J., Riley, G. W., Barndt, J. K., Berry, J. R., . . . Khan,
M. A. (1995). Stratigraphic evidence for an early collision between northwest India and
Asia. *Nature*, 373(6509), 55-58.
- Burg, J. P., Leyreloup, A., Girardeau, J., & Chen, G. M. (1987). Structure and Metamorphism of a
Tectonically Thickened Continental Crust: The Yalu Tsangpo Suture Zone (Tibet).
Philosophical Transactions of the Royal Society of London. Series A, Mathematical and

306 *Physical Sciences*, 321(1557), 67-86.

307 Chenet, A., Quidelleur, X., Fluteau, F., Courtillot, V., & Bajpai, S. (2007). 40K–40Ar dating of the
 308 Main Deccan large igneous province: Further evidence of KTB age and short duration.
 309 *Earth and Planetary Science Letters*, 263(1-2), 1-15.

310 Contreras-Reyes, E., Flueh, E. R., & Grevenmeyer, I. (2010). Tectonic control on sediment
 311 accretion and subduction off south-central Chile. *Tectonics*, 29(6). doi:
 312 10.1029/2010TC002734

313 Copley, A., Avouac, J.-P., & Royer, J.-Y. (2010). India-Asia collision and the Cenozoic slowdown
 314 of the Indian plate: Implications for the forces driving plate motions. *Journal of*
 315 *Geophysical Research: Solid Earth*, 115, B03410. doi:10.1029/2009JB006634

316 DeCelles, P. G., Kapp, P., Gehrels, G. E., & Ding, L. (2014). Paleocene-Eocene foreland basin
 317 evolution in the Himalaya of southern Tibet and Nepal: Implications for the age of initial
 318 India-Asia collision. *Tectonics*, 33(5), 824-849.

319 Ding, L., Kapp, P., & Wan, X. (2005). Paleocene-Eocene record of ophiolite obduction and initial
 320 India-Asia collision, south central Tibet. *Tectonics*, 24(3), TC3001.
 321 doi:10.1029/2004TC001729.

322 Garzanti, E. (2019). Petrographic classification of sand and sandstone. *Earth-Science Reviews*, 192,
 323 545-563.

324 Garzanti, E., Baud, A., & Mascle, G. (1987). Sedimentary Record of the Northward Flight of India
 325 and Its Collision with Eurasia (Ladakh Himalaya, India). *Geodinamica Acta*, 1(4-5),
 326 297-312.

327 Garzanti, E., & Hu, X. (2015). Latest Cretaceous Himalayan tectonics: Obduction, collision or

328 Deccan-related uplift? *Gondwana Research*, 28(1), 165-178. doi:10.1016/j.gr.2014.03.010

329 Gehrels, G., Kapp, P., DeCelles, P., Pullen, A., Blakey, R., Weislogel, A., Ding, L., Guynn, J.,
330 Martin, A., McQuarrie, N., & Yin, A. (2011). Detrital zircon geochronology of pre-Tertiary
331 strata in the Tibetan-Himalayan orogen. *Tectonics*, 30(5), TC5016.
332 doi:10.1029/2011TC002868

333 Hu, X., An, W., Wang, J., Garzanti, E., & Guo, R. (2014). Himalayan detrital chromian spinels and
334 timing of Indus-Yarlung ophiolite erosion. *Tectonophysics*, 621, 60-68.

335 Hu, X., Garzanti, E., Moore, T., & Raffi, I. (2015). Direct stratigraphic dating of India-Asia
336 collision onset at the Selandian (middle Paleocene, 59 ± 1 Ma). *Geology*, 43(10), 859-862.

337 Hu, X., Garzanti, E., Wang, J., Huang, W., An, W., & Webb, A. (2016). The timing of India-Asia
338 collision onset – Facts, theories, controversies. *Earth-Science Reviews*, 160, 264-299.

339 Hu, X., Jansa, L., Chen, L., Griffin, W.L., O'Reilly, S.Y., & Wang, J.G. (2010). Provenance of
340 Lower
341 Cretaceous Wolong Volcaniclastics in the Tibetan Tethyan Himalaya: implications for
342 the final breakup of Eastern Gondwana. *Sedimentary Geology*, 223 (3-4), 193-205.

343 Hu, X., Sinclair, H. D., Wang, J., Jiang, H., & Wu, F. (2012). Late Cretaceous-Palaeogene
344 stratigraphic and basin evolution in the Zhepure Mountain of southern Tibet: implications
345 for the timing of India-Asia initial collision. *Basin Research*, 24(5), 520-543.

346 Hu, X., Wang, J., An, W., Garzanti, E., & Li, J. (2017). Constraining the timing of the India-Asia
347 continental collision by the sedimentary record. *Science China Earth Sciences*, 60(4),
348 603-625.

349 Hubert, J. (1962). A Zircon-Tourmaline-Rutile Maturity Index and the Interdependence of the

350 Composition of Heavy Mineral Assemblages with the Gross Composition and Texture of
 351 Sandstones. *Journal of Sedimentary Research*, 32.
 352 doi:10.1306/74D70CE5-2B21-11D7-8648000102C1865D

353 Ji, W. Q., Wu, F. Y., Chung, S. L., Li, J. X., & Liu, C. Z. (2009). Zircon U–Pb geochronology and
 354 Hf isotopic constraints on petrogenesis of the Gangdese batholith, southern Tibet. *Chemical*
 355 *Geology*, 262(3-4), 229-245.

356 Kamenetsky, V. S., Crawford, A. J., & Meffre, S. (2001). Factors Controlling Chemistry of
 357 Magmatic Spinel: an Empirical Study of Associated Olivine, Cr-spinel and Melt Inclusions
 358 from Primitive Rocks. *Journal of Petrology*, 42(4), 655-671.

359 Kapp, P., & Decelles, P. (2019). Mesozoic-Cenozoic geological evolution of the
 360 Himalayan-Tibetan orogen and working tectonic hypotheses. *American Journal of Science*,
 361 319, 159-254.

362 Leech, M. L., Singh, S., Jain, A. K., Klemperer, S. L., & Manickavasagam, R. M. (2005). The
 363 onset of India-Asia continental collision: Early, steep subduction required by the timing of
 364 UHP metamorphism in the western Himalaya. *Earth and Planetary Science Letters*,
 365 234(1-2), 83-97.

366 Li, J., Hu, X., Garzanti, E., Banerjee, S., BouDagher Fadel, M. (2020). Late Cretaceous
 367 topographic doming caused by initial upwelling of Deccan magmas: Stratigraphic and
 368 sedimentological evidence. *Geological Society of America Bulletin*,
 369 <https://doi.org/10.1130/B35133.1>

370 Li, X., Wang, C., & Hu, X. (2005). Stratigraphy of deep-water Cretaceous deposits in Gyangze,
 371 southern Tibet, China. *Cretaceous Research*, 26(1), 33-41.

372 Li, Y., Wang, C., Hu, X., Bak, M., Wang, J., & Chen, L. (2007). Characteristics of Early Eocene
 373 radiolarian assemblages of the Saga area, southern Tibet and their constraint on the closure
 374 history of the Tethys. *Chinese Science Bulletin*, 52, 2108-2114.

375 Metcalf, K., & Kapp, P. (2017). The Yarlung suture mélange, Lopu Range, southern Tibet:
 376 Provenance of sandstone blocks and transition from oceanic subduction to continental
 377 collision. *Gondwana Research*, 48, 15-33.

378 Molnar, P., Boos, W. R., & Battisti, D. S. (2010). Orographic Controls on Climate and
 379 Paleoclimate of Asia: Thermal and Mechanical Roles for the Tibetan Plateau. *Annual
 380 Review of Earth and Planetary Sciences*, 38(1), 77-102.

381 Mutti, E., Davoli, G., petroli, A. g. i., & geologia, U. d. P. I. d. (1992). *Turbidite sandstones*: Agip,
 382 Istituto di geologia, Università di Parma.

383 Najman, Y., Appel, E., Boudagher-Fadel, M., Bown, P., Carter, A., Garzanti, E., Godin, L., Han, J.,
 384 Liebke, U., Oliver, G., Parrish, R., & Vezzoli, G. (2010). Timing of India-Asia collision:
 385 Geological, biostratigraphic, and palaeomagnetic constraints. *Journal of Geophysical
 386 Research: Solid Earth*, 115, B12416. doi:10.1029/2010jb007673

387 Najman, Y., Jenks, D., Godin, L., Boudagher-Fadel, M., Millar, I., Garzanti, E., Horstwood, M., &
 388 Bracciali, L. (2017). The Tethyan Himalayan detrital record shows that India–Asia terminal
 389 collision occurred by 54 Ma in the Western Himalaya. *Earth and Planetary Science Letters*,
 390 459, 301-310.

391 Nicora, A., Garzanti, E., & Fois, E. (1987). Evolution of the Tethys Himalaya continental shelf
 392 during Maastrichtian to Paleocene (Zaskar, India). *Rivista Italiana di Paleontologia e
 393 Stratigrafia*, 92, 439–496.

- 394 Pan, G., Ding, J., Yao, D., & Wang, L. (2004). *The Guide Book of 1:1,500,000 Geologic Map of*
 395 *the Qinghai-Xizang (Tibet) Plateau and Adjacent Areas*. Chengdu Map Publishing
 396 Company, Chengdu.
- 397 Rowley, D. B. (1996). Age of initiation of collision between India and Asia: A review of
 398 stratigraphic data. *Earth and Planetary Science Letters*, 145(1), 1-13.
- 399 van Hinsbergen, D. J., Lippert, P. C., Dupont-Nivet, G., McQuarrie, N., Doubrovine, P. V.,
 400 Spakman, W., & Torsvik, T. H. (2012). Greater India Basin hypothesis and a two-stage
 401 Cenozoic collision between India and Asia. *Proceedings of the National Academy of*
 402 *Sciences*, 109(20), 7659-7664.
- 403 Wang, J., Hu, X., Jansa, L., & Huang, Z. (2011). Provenance of the Upper Cretaceous–Eocene
 404 Deep-Water Sandstones in Sangdanlin, Southern Tibet: Constraints on the Timing of Initial
 405 India-Asia Collision. *The Journal of Geology*, 119(3), 293-309.
- 406 Wu, F., Ji, W., Wang, J., Liu, C., Chung, S., & Clift, P. D. (2014). Zircon U–Pb and Hf isotopic
 407 constraints on the onset time of India-Asia collision. *American Journal of Science*, 314(2),
 408 548-579.
- 409 Yin, A., & Harrison, T. M. (2000). Geologic evolution of the Himalayan-Tibetan orogen. *Annual*
 410 *Review of Earth and Planetary Sciences*, 28(1), 211-280.
- 411 Yuan, J., Yang, Z., Deng, C., Krijgsman, W., Hu, X., Li, S., Shen, Z., Qin, H., An, W., He, H., Ding,
 412 L., Guo, Z., & Zhu, R. (2020). Rapid drift of the Tethyan Himalaya terrane before
 413 two-stage India-Asia collision. *National Science Review*. doi:10.1093/nsr/nwaa173